ADVANCED MATERIALS
www.advmat.de

Materials Views
www.MaterialsViews.com

# Aqueous-Processable Noncovalent Chemically Converted Graphene–Quantum Dot Composites for Flexible and Transparent Optoelectronic Films

By *Xiumei Geng, Liang Niu, Zhenyuan Xing, Rensheng Song, Guangtong Liu, Mengtao Sun, Guosheng Cheng,* Haijian Zhong, Zhenghui Liu, Zhijun Zhang, Lianfeng Sun, Hongxing Xu, Li Lu,* and *Liwei Liu**

Graphene, as an atomic-layer-thick 2D system, has triggered considerable research interests since the pioneer exfoliation preparation.[1] It has been demonstrated that graphene has many unique electronic properties, such as massless Dirac fermions, the quantum hall effect, and spin-dependent transport at room temperature.[2–4] The high field-effect mobility and the superior thermal conductivity of individual graphene were also reported.[5,6] These fascinating properties of graphene hold promising potential for electronic devices, sensitive chemical sensors, thermal management, and composite materials.[7–12] However, perfect graphene does not show evident advantages in optoelectronics owing to its nature as a zero-bandgap semiconductor.[13]

Semiconductor nanocrystals, known as quantum dots (QDs), show unique size-dependent optical absorption compared with their bulk counterparts.[14,15] QDs have been intensively investigated for their significant potential in biological fluorescent labels and optoelectronic devices.[16,17] QDs are usually coated with organic ligands to prevent aggregation and chemical degradation. Nonetheless, the coating organic-ligand layer severely limits the conductivity and the photoconductivity of QD-array films because of the influence of the ligands on the interactions and the spatial distribution of nanopaticles.[18,19] This severely encumbers the applications of QDs in optoelectronic devices.

Large-scale production of perfect graphene has hitherto been lacking. Recently, several groups obtained graphene using solution-phase methods, allowing for scalable and composites feasible graphene.[20–24] The enhanced electrical, mechanical, and thermal properties have, thus, been demonstrated in graphene–polymer composites.[25,26] In addition, $TiO_2$ nanoparticles, blending directly with graphite oxide, were used to exhibit a method of UV-assisted photocatalytic reduction.[27] Furthermore, the reduced graphite-oxide films have been obtained by spin-coating or mechanical transfer as a flexible and transparent electrical material.[28,29] However, fabrication and properties of flexible chemically converted graphene (CCG) and QD composites remain to be investigated urgently for their optoelectronic and energy conversion applications.

Here, we have prepared composites of CCG and CdSe QDs (graphene–quantum dots, GQs) via π–π stacking of aromatic structures between CCG and CdSe QDs capped with Pyridine (Py). The flexible and transparent optoelectronic films fabricated from the composites show improved photosensitivity with increasing loadings of QDs. Charge transfer from the QDs to the CCG under illumination is confirmed by the change in the photoconductivities of GQ films with increasing loadings of QDs. Moreover, the photoconductivity of GQ films is significantly higher than that of the treated intrinsic CdSe QD array film.

We propose a synthetic strategy for GQs composites, as shown in Scheme 1. CCG was prepared by reducing graphite oxide using a modified Hummers method.[30,31] Trioctylphosphine oxide (TOPO)-capped CdSe QDs were synthesized by a solution-chemical route developed by Peng and co-workers and Weller and co-workers.[32,33] TOPO ligands of CdSe QDs were almost completely exchanged with Py by repeatedly refluxing in anhydrous Py (Fig. 1a). Subsequently, the GQ-composite materials were synthesized by mixing water-diluted CCG with Py-capped QDs in aqueous solution (see Supporting Information). Py plays multiple roles, simultaneously. Firstly, Py-capped CdSe QDs are soluble in polar solvents, which meets the requirement of producing composite as CCG is soluble in water. Secondly, not only is Py expected to introduce a π–π stacking interaction between CCG and QDs but also the small Py molecule should favor the charge transfer between two components. The attachment of CdSe QDs to CCG is evidenced by observation of precipitation when higher-concentrated CdSe QDs are added into the CCG solution. Stable solutions of GQ composites are obtained by adding lower-concentrated CdSe QDs into the CCG solution; the solution remains clear for several weeks (Fig. 1b). Attachment of QDs to CCG is further supported by transmission electron microscopy (TEM) and electrical measurements. In addition, we also find that Py has a steric function stabilizing CCG

[*] Prof. G. Cheng, Prof. L. Liu, X. Geng, L. Niu, Z. Xing, R. Song, H. Zhong, Dr. Z. Liu, Prof. Z. Zhang
Suzhou Institute of Nano-Tech and Nano-Bionics, Chinese Academy of Sciences
Suzhou 215125 (P. R. China)
E-mail: gscheng2006@sinano.ac.cn; lwliu2007@sinano.ac.cn
Prof. G. Liu, Prof. M. Sun, Prof. H. Xu, Prof. L. Lu
Institute of Physics, Chinese Academy of Sciences
Beijing 100190 (P. R. China)
Prof. L. Sun
National Center for Nanoscience and Technology
Beijing 100190 (P. R. China)

DOI: 10.1002/adma.200902871

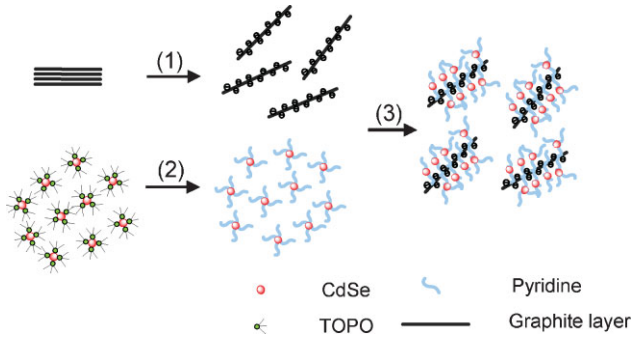


**Scheme 1.** Schematic image illustrating the formation of CCG–QDs composite materials: (1) Graphite oxide was dispersed ultrasonically and reduced graphite oxide was stabilized in aqueous solution by electrostatic interaction. (2) TOPO ligands of as-prepared CdSe QDs were exchanged with Py, and Py-capped CdSe quantum dots were dispersed in aqueous solution. (3) The composite of CCG and CdSe QDs was formed in aqueous solution.

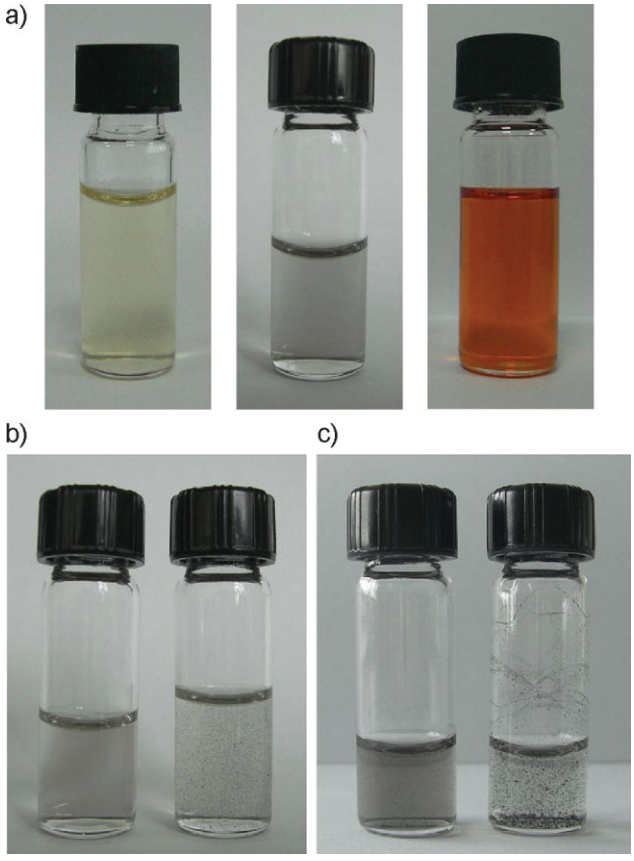


**Figure 1.** a) Solutions of graphite oxide, CCG, and Py-capped CdSe QDs. b) Comparison of composite solutions made from CCG and different concentrations of QDs. A precipitation effect occurred when adding high-concentrated QDs (right vial), while the composite solution was stable when adding low-concentrated QDs (left vial). c) Steric effect of Py stabilizing the CCG solution, tested by salt effects. Precipitation occurred in aqueous CCG solution without Py after adding a salt solution (right vial), while an aqueous CCG solution with Py remains stable when adding a salt solution (left vial).

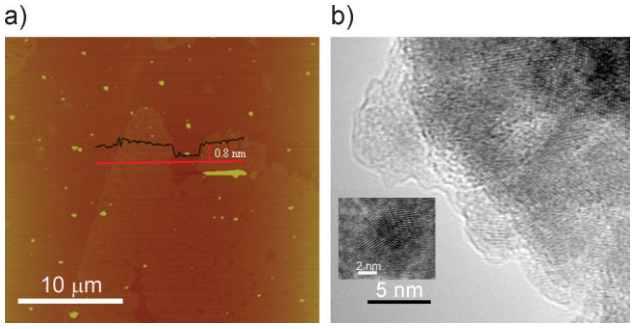


**Figure 2.** a) AFM images of separated CCG flakes on a silicon substrate. b) High-resolution TEM image of GQ composites. The inset shows the TEM image of an individual CdSe QD with a particle size of ~4 nm.

in solution, which is confirmed by the salt effect in parallel experiments. Precipitation occurs instantly in aqueous CCG solution without Py when a salt solution is added, while an aqueous CCG solution with Py is stable for several hours after adding a salt solution (Fig. 1c). This will play important roles in stabilizing CCG and demonstrating the solution-processed advantages.

To indicate the acquirement of single-sheet CCG, an aqueous solution of CCG was dropped onto the hydrophilic-treated silicon for atomic force microscopy (AFM) measurements. Figure 2a shows an AFM image of CCG on the silicon substrate; the thickness of the sheet is equal to or less than 1 nm. Large-area graphene with lateral sizes of more than a few tens of micrometers can be obtained by low-power ultrasonication and centrifugation.

For TEM sample preparation, a small quantity of GQs composite solution was dropped onto the 300 mesh copper TEM grid. TEM images were obtained from samples attached on the edge the of copper grid, avoiding the complicated lithography process of fabricating micrometer-sized metallic grids. The lattices of CdSe QDs covering the graphene layers are cleanly seen in the high-resolution TEM image (Fig. 2b). The inset shows a TEM image of an individual CdSe QDs with a diameter of ~4 nm.

To explore practical applications, it is essential to achieve films of CCG and GQ composite using solution-processed methods. The filtered films of CCG and GQ composite were prepared by vacuum filtration through a mixed cellulose–ester membrane with a pore size of 0.1 μm. The thickness of films is easily controlled by varying the volume of the suspensions. The as-prepared filtered films of CCG and GQs can be readily transferred onto plastic and rigid substrates by mechanical pressing. Figure 3a–d shows the optical images of the filtered films and transferred films. Figure 3d shows a photograph of a typical device made of flexible, transparent, and conducting GQs film with patterned Au electrodes of 100 nm deposited by thermal shadow evaporation.

We compare the absorbance spectra of CCG, GQs thin films on transparent substrates, and TOPO-capped CdSe QDs in hexane solution. The absorbance peak appearing in GQ films corresponds to the excitation peak of CdSe QDs with a small redshift (Fig. 4a). It is worth noting that overloading QDs into CCG solution will lead to a partial peeling of the transferred composite films off the plastic substrates, resulting from the precipitation of

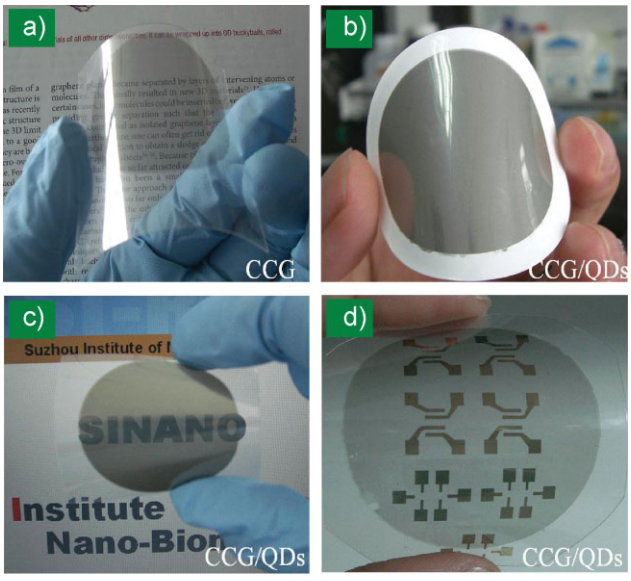


**Figure 3.** Optical photographs and optical properties of CCG and GQs films. a) A transferred CCG film on a PET substrate. b) A filtered GQ composite film on mixed cellulose ester membrane. c) A transferred GQ composite film on plastic substrate. d) A GQ film with patterned electrodes on a flexible and transparent plastic substrate.

composites in solution and possible excess layers of QDs attaching to the CCG flakes. Thin composite films of GQs can be transferred onto transparent substrates and show a transmittance of up to 92% (Fig. 4b). Reflection spectra of CCG and GQs films were recorded to show the absorption features of QDs in composite films (see Supporting Information, Fig. S4).

Electronic and optoelectronic characteristics of the devices fabricated from GQ films on plastic substrates were measured by a four-probe method under ambient conditions. Figure 5a shows typical four-probe current–voltage curves of an annealed GQ composite film with an average film thickness of ~126.7 nm (0.28 mg CCG/0.4 mg QDs) under dark conditions and laser irradiation. The annealing is performed in a quartz tube with hydrogen gas protection at 150 °C for 26 h. The current versus voltage characteristic is linear and symmetric within the measured range. Exposing the annealed composite film of ~126.7-nm thickness (0.28 mg CCG/0.4 mg QDs) to 473-nm laser irradiation of ~94.5 mW resulted in a rise in conductance of ~10.5%. To reveal the effect of QDs on the photoresponse in GQ films, a series of GQ composite films were prepared remaining a constant quantity of CCG and increasing the loadings of QDs. Figure 5b shows the change of photoconductivities with various loadings of QDs in annealed composite films obtained by four-probe measurements under a constant current of 100 μA. Photoconductivities rise with an increasing amount of QDs at the lower loadings of QDs in the GQ composite films, and photoconductivity finally decreases to a lower value at higher loading of QDs. It is noted that the annealed samples are highly stable, even after exposure to air for several weeks. We also investigated the annealing effect of the composite films (Fig. S5).

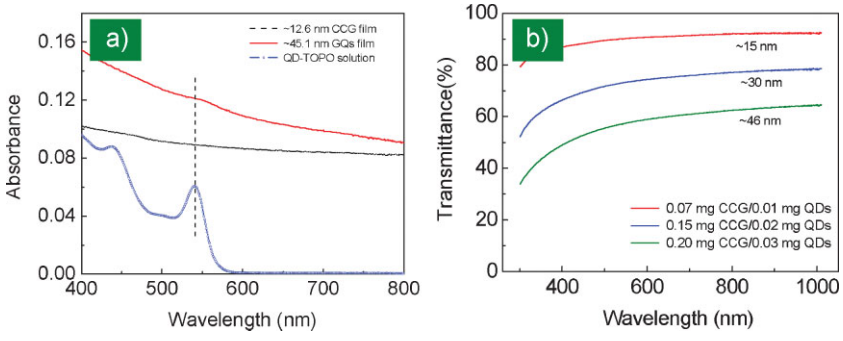


**Figure 4.** a) The absorbance of CCG and GQ films (0.18 mg CCG/0.10 mg QDs) on a transparent substrate and TOPO-capped CdSe QDs in hexane solution. b) Transmittance of various GQs films with indicated film thicknesses.

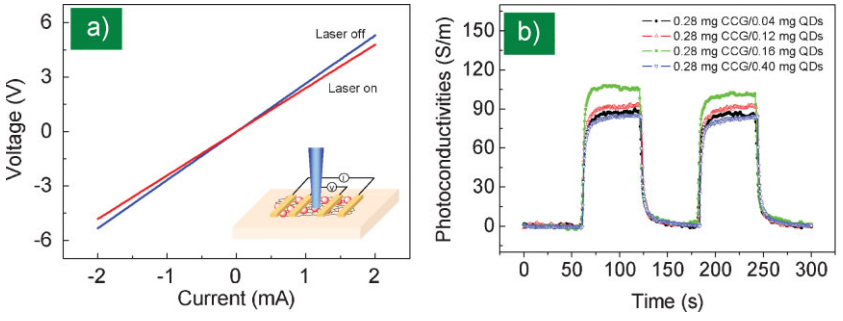


**Figure 5.** Electrical and optoelectronic-property measurements on the plastic substrates. a) Current–voltage characteristics measured by a four-probe method for ~126.67 nm (0.28 mg CCG/0.4 mg QDs) film on a flexible substrate with and without laser irradiation. The inset shows the configuration of the measurement. b) The photoconductivity switching changes under the bias of 100 μA and 94.5 mW irradiation in various composite films of 0.28 mg CCG/0.04 mg QDs, 0.28 mg CCG/0.12 mg QDs, 0.28 mg CCG/0.16 mg QDs, and 0.28 mg CCG/0.40 mg QDs with an average film thickness of 68.57, 75.65, 86.80, and 126.67 nm, respectively.

From the theoretical point of a photoconductor, the photoconductivity, $\sigma_{ph}$, of a film is generally proportional to the number of photogenerated carriers $\Delta n$ and the mobility of carriers $\mu$, given by $\sigma_{ph} = \frac{e \cdot \Delta n \cdot \mu}{W \cdot d \cdot L}$, where $L$, $W$, $d$, and $e$ are length, width, and thickness of the film, and the electronic charge. The change of photoconductivities is consistent with the expected consequence that adding of QDs leads to a competition between increasing photogenerated carriers and reducing the mobility of carriers. Furthermore, the charge transfer from QDs to CCG increasing photogenerated carriers can be confirmed by the observed increase in photoconductivity with increasing loadings of QDs. Considering the photoelectrical conversion process, we believe that the introduction of QDs to the CCG films will degrade dark photoconductivity of the system and will enhance the absorption and the number of photogenerated carriers. Therefore, the photosensitivity defined by the ratio of photoconductivity to dark conductivity should be improved for composite film. We do find the improvement in photosensitivity and a decrease of dark conductivity by increasing the

loadings of QDs in composites (Table S1). For instance, the changes of photosensitivity are ~3.08% and ~9.10% for the composite films of 0.28 mg CCG/0.04 mg QDs and 0.28 mg CCG/0.4 mg QDs, respectively.

Further analysis shows that photoconductivities of the GQ films are much higher than those of the intrinsic CdSe QD array films. In general, a CdSe QD film is highly insulating and its photoconductivity is almost undetectable. The improved photoconductivity of intrinsic films of CdSe QDs treated with NaOH is reported to be $\sim 10^{-10}$ S m$^{-1}$ under 14 mW cm$^{-2}$ excitation intensity.[19] By contrast, the photoconductivity in an annealed composite film of ~86.8-nm thickness (0.28 mg CCG/0.16 mg QDs) is observed to be $\sim 10^{2}$ S m$^{-1}$ under an excitation intensity of ~3150 mW cm$^{-2}$. Considering the general linear increase in photoconductivity with excitation intensity, we derive that the photoconductivity of the composite film will be more than 10 orders of magnitude higher than that of the treated CdSe QDs films upon further optimization. This indicates potential for improving the performance of QDs-based optoelectronic devices.

In summary, we successfully fabricated composite films via noncovalent coupling of CdSe QDs to CCG in aqueous solutions. The optoelectronic properties of flexible and transparent transferred GQ films have been investigated. The photosensitivity of the composites was improved ~3 folds by introduction of QDs. The photoconductivity of the composite film can be up to ~10 orders of magnitude higher than that of intrinsic CdSe QD films and there is still room to improve. The results presented here offer a new route of preparing CCG–QD composite materials, which is promising for new active or electrode materials in optoelectronic devices. The thin GQ composite films enable the fabrication of large-area flexible and transparent optoelectronic devices by the facile solution processing method.

## Experimental

*Preparation of CCG, QDs, and Their Composites*: Brown graphite oxide was prepared from natural graphite powder (300 mesh, Alfa Aesar) by a modified Hummers method [30,31]. CCG was prepared and dispersed in water using Li's method [19]. CdSe QDs was synthesized by a similar method developed by Peng [32] and Weller [33]. TOPO ligands of CdSe QDs were exchanged with Py by refluxing in anhydrous Py at 118 °C under argon for 24 h. CdSe QDs were then precipitated by adding hexane followed by centrifugation. The precipitated CdSe was redissolved in Py and stirred at 65 °C for 1 h; the exchange process including precipitation and dissolution was repeated three times so that the TOPO was almost completely exchanged with Py. Subsequently, the GQ composite materials were synthesized by mixing water-diluted CCG with Py-capped QDs in aqueous solution. The concentrations of CCG and QDs solutions were obtained by measuring the residual solute after evaporation of the solvent so that the quantity of CCG and QDs can be determinated. The detailed protocol for synthesis and fabrication of the films is described in the Supporting Information.

*Characterization of Optical and Electrical Properties*: The average thicknesses of films were determined by the repeated AFM (Digital Instrument Dimension 3100, Vecco) measurements. Electron transport and optoelectronic measurements were carried out in air and at room temperature for the GQs films on flexible transparent substrates. The length of the electrodes was 3 mm and the spacing of the center electrodes is 1 mm, which is the area measured by the four-probe method with an Agilent semiconductor parameter analyzer B1500A. A solid state 473-nm semiconductor diode pumped laser was used as excitation light source in consideration of excitation of CdSe QDs. The laser with excitation power of 100 mW was placed 15 cm away from the sample and the laser power applied to the sample is ~94.5 mW measured with a PD300-UV photodiode head and a Laserstar power meter. By adjusting the light beam, the whole measured area of the sample can be illuminated. UV–vis absorption and transmission spectra were recorded with a Perkin Elmer Lambda 25 spectrophotometer.

## Acknowledgements

This work was supported by the National Natural Science Foundation of China (Grant Nos. 10974141, 10774172, 90923003), the Suzhou Science and Technology Development Plan, and the Key Program of the National Science Foundation of China (Award ID: 10834004). L.W.L. thanks the Platforms of Characterization & Test and Nanofabrication Facility at Sinano for experimental assistance. Supporting Information is available online from Wiley InterScience or from the author.

Received: August 25, 2009
Published online: November 30, 2009

[1] K. S. Novoselov, A. K. Geim, S. V. Morozov, D. Jiang, Y. Zhang, S. V. Dubonos, I. V. Grigorieva, A. A. Firsov, *Science* **2004**, *306*, 666.
[2] K. S. Novoselov, A. K. Geim, S. V. Morozov, D. Jiang, M. I. Katsnelson, I. V. Grigorieva, S. V. Dubonos, A. A. Firsov, *Nature* **2005**, *438*, 197.
[3] K. S. Novoselov, Z. Jiang, Y. Zhang, S. V. Morozov, H. L. Stormer, U. Zeitler, J. C. Maan, G. S. Boebinger, P. Kim, A. K. Geim, *Science* **2007**, *315*, 1379.
[4] N. Tombros, C. Jozsa, M. Popinciuc, H. T. Jonkman, B. J. van Wees, *Nature* **2007**, *448*, 571.
[5] A. K. Geim, K. S. Novoselov, *Nat. Mater.* **2007**, *6*, 183.
[6] A. A. Balandin, S. Ghosh, W. Z. Bao, I. Calizo, D. Teweldebrhan, F. Miao, C. N. Lau, *Nano Lett.* **2008**, *8*, 902.
[7] X. R. Wang, Y. J. Ouyang, X. L. Li, H. L. Wang, J. Guo, H. J. Dai, *Phys. Rev. Lett.* **2008**, *100*, 206803.
[8] P. Blake, P. D. Brimicombe, R. R. Nair, T. J. Booth, D. Jiang, F. Schedin, L. A. Ponomarenko, S. V. Morozov, H. F. Gleeson, E. W. Hill, A. K. Geim, K. S. Novoselov, *Nano Lett.* **2008**, *8*, 1704.
[9] F. Schedin, A. K. Geim, S. V. Morozov, E. W. Hill, P. Blake, M. I. Katsnelson, K. S. Novoselov, *Nat. Mater.* **2007**, *6*, 652.
[10] M. D. Stoller, S. J. Park, Y. W. Zhu, J. H. An, R. S. Ruoff, *Nano Lett.* **2008**, *8*, 3498.
[11] W. Xuan, L. J. Zhi, M. Klaus, *Nano Lett.* **2008**, *8*, 323.
[12] Z. F. Liu, Q. Liu, Y. Huang, Y. F. Ma, S. G. Yin, X. Y. Zhang, W. Sun, Y. S. Chen, *Adv. Mater.* **2008**, *20*, 3924.
[13] E. J. H. Lee, K. Balasubramanian, R. T. Weitz, M. Burghard, K. Kern, *Nat. Nanotechnol.* **2008**, *3*, 486.
[14] C. B. Murray, D. J. Norris, M. G. Bawendi, *J. Am. Chem. Soc.* **1993**, *115*, 8706.
[15] A. P. Alivisatos, *J. Phys. Chem.* **1996**, *100*, 13226.
[16] M. Bruchez, Jr, M. Moronne, P. Gin, S. Weiss, A. P. Alivisatos, *Science* **1998**, *281*, 2013.
[17] W. U. Huynh, J. J. Dittmer, A. P. Alivisatos, *Science* **2002**, *295*, 2425.
[18] N. Y. Morgan, C. A. Leatherdale, M. Drndić, M. V. Jarosz, M. A. Kastner, M. G. Bawendi, *Phys. Rev. B* **2002**, *66*, 075339.
[19] M. V. Jarosz, V. J. Porter, B. R. Fisher, M. A. Kastner, M. G. Bawendi, *Phys. Rev. B* **2004**, *70*, 195327.
[20] D. Li, M. B. Muller, S. Gilje, R. B. Kaner, G. G. Wallace, *Nat. Nanotechnol.* **2008**, *3*, 101.
[21] X. L. Li, G. Y. Zhang, X. D. Bai, X. M. Sun, X. R. Wang, E. G. Wang, H. J. Dai, *Nat. Nanotechnol.* **2008**, *3*, 538.
[22] Y. Hernandez, V. Nicolosi, M. Lotya, F. M. Blighe, Z. Y. Sun, S. De, I. T. Mcgovern, B. Holland, M. Byrne, Y. K. Gun'Ko, J. J. Boland, P. Niraj,

G. Duesberg, S. Krishnamurthy, R. Goodhue, J. Hutchison, V. Scardaci, A. C. Ferrari, J. N. Coleman, *Nat. Nanotechnol.* **2008**, *3*, 563.
[23] Y. C. Si, E. T. Samulski, *Nano Lett.* **2008**, *8*, 1679.
[24] V. C. Tung, M. J. Allen, Y. Yang, R. B. Kaner, *Nat. Nanotechnol.* **2009**, *4*, 25.
[25] S. Stankovich, D. A. Dikin, G. H. B. Dommett, K. M. Kohlhaas, E. J. Zimney, E. A. Stach, R. D. Piner, S. T. Nguyen, R. S. Ruoff, *Nature* **2006**, *442*, 282.
[26] T. Ramanathan, A. A. Abdala, S. Stankovich, D. A. Dikin, M. Herrera-Alonso, R. D. Piner, D. H. Adamson, H. C. Schniepp, X. Chen, R. S. Ruoff, S. T. Nguyen, *Nat. Nanotechnol.* **2008**, *3*, 327.
[27] G. Williams, B. Seger, P. V. Kamat, *ACS Nano* **2008**, *2*, 1487.
[28] H. A. Becerril, J. Mao, Z. F. Liu, R. M. Stoltenberg, Z. N. Bao, Y. S. Chen, *ACS Nano* **2008**, *2*, 463.
[29] G. Eda, G. Fanchini, M. Chhowalla, *Nat. Nanotechnol.* **2008**, *3*, 270.
[30] W. S. Hummers, Jr, R. E. Offeman, *J. Am. Chem. Soc.* **1958**, *80*, 1339.
[31] N. I. Kovtyukhova, P. J. Ollivier, B. R. Martin, T. E. Mallouk, S. A. Chizhik, E. V. Buzaneva, A. D. Gorchinskiy, *Chem. Mater.* **1999**, *11*, 771.
[32] L. H. Qu, X. G. Peng, *J. Am. Chem. Soc.* **2002**, *124*, 2049.
[33] B. H. Juarez, C. Klinke, A. Kornowski, H. Weller, *Nano Lett.* **2007**, *7*, 3564.